

Evaluation of demineralized lignin and lignin-phenolic resin blends to produce biocoke suitable for blast furnace operation

Miguel Castro-Díaz^{a,*}, María Fernanda Vega^b, Elvira Díaz-Faes^b, Carmen Barriocanal^b,
Umaru Musa^a, Colin Snape^a

^a Department of Chemical and Environmental Engineering, University of Nottingham,
Faculty of Engineering, Energy Technologies Building, Nottingham NG7 2TU, United
Kingdom

^b Instituto Nacional del Carbón, INCAR-CSIC, Apartado 73, 33080 Oviedo, Spain

Abstract

Metallurgical coke makers could reduce carbon emissions and material costs by introducing waste lignin in coke oven charges. Two approaches have been studied here to increase the use of lignin in the preparation of metallurgical coke: lignin demineralization with H₂SO₄ and lignin blending with a low rank coal using phenolic resin as binder. The biocoke obtained after carbonization at 1000 °C from the hydrochar of demineralized lignin (350 °C, 6 h, biomass/water=0.5 wt/wt) had much higher reactivity than the coke obtained from the low rank coking coal, proving that demineralization of lignin prior hydrothermal conversion is not a valid route for biocoke

* Corresponding author.

E-mail address: miguel.castro@nottingham.ac.uk (M. Castro-Díaz)

making. In the other approach, it was found that blends containing 70 wt% low rank coal, 24 wt% torrefied lignin (before or after demineralization) and 6 wt% phenolic resin produced biocokes with suitable mechanical strength for handling but higher reactivity than the coke obtained from the low rank coking coal alone. The microporous surface areas of the biocokes studied did not correlate with their reactivity values.

Keywords: Kraft lignin, demineralization, torrefaction, phenolic resin, biocoke.

1. Introduction

Scarcity of prime coals for metallurgical coke making and more stringent reduction targets for carbon emissions are two main challenges facing the steel industry. Consequently, coke makers and steel producers must seek ways of lowering CO₂ emissions and decrease production costs without seriously undermining process efficiency. The use of readily available biomass materials offers the advantages of reducing non-renewable carbon emissions and reducing material costs. However, partial replacement of metallurgical, or coking, coals with biomass materials to produce biocoke in industrial coke ovens is limited by the deleterious effects of biomass on biocoke reactivity, mechanical strength and yield. For instance, the use of wood charcoal in integrated steelworks is limited by: i) its negative impact on coke quality when added to coking coal blends; ii) its low mechanical strength that cannot support the iron ore burden in large blast furnaces; iii) its low abrasion resistance; and iv) its ash chemistry that can accelerate its reactivity towards CO₂ in the blast furnace. Subsequently, the highest amount of pristine or thermally treated biomass that can be added to a coal blend while maintaining biocoke quality suitable for blast furnace operation is 5 wt% [1]. Recently, Xing et al. [2] introduced 7.5 wt% charcoal in a coal blend using coal tar pitch (2 wt%) as binder. These authors attributed the high reactivity of the resultant biocoke to the combined effect of an increase in the interfacial reaction area (i.e. higher surface area) due to the presence of charcoal and the promotion of gasification reactions by the alkali and alkaline earth metals in charcoal. The higher reactivity created voids and caused coalescence of pores in the biocoke, resulting in lower mechanical strength. Therefore, production of biocoke with suitable mechanical stability and reactivity for the blast furnace operation is still a challenging task.

57

58 Kraft lignin is a renewable polymer that is obtained as a by-product in the pulping
59 industry. In a recent work, Suopajarvi et al. [3] studied the effect of Kraft lignin
60 addition on coke compression strength and reactivity. Addition of Kraft lignin reduced
61 the biocoke mechanical strength (2.5 wt% addition lowered the strength by 26.3%) and
62 increased its reactivity compared to the reference coke. The reduction in mechanical
63 strength of the biocoke could be partly attributed to the evolution of volatiles from
64 lignin (>50 wt%) that may cause the shrinkage of the solid particles and lead to the
65 development of fissures, cracks and new pores.

66

67 The possible conversion of Kraft lignin into biocoke through hydrothermal
68 carbonization was investigated by our research group [4]. The hydrochars obtained at
69 350 °C for 6 h using 30 mL of water from pine Kraft lignin, torrefied lignin and a 50:50
70 wt/wt blend of pristine and torrefied lignins yielded less ash than a good coking coal
71 (i.e. <2 wt% cf. 10 wt%). However, the reactivity of the biocokes obtained after
72 carbonization was excessively high compared to that of the coke from the good coking
73 coal (>45% cf. 10%) and the mechanical strength of the biocokes was much lower than
74 that of the coke. The high total porosity of the biocokes (>39%) and their high
75 microporous surface areas (>400 m²/g) compared to those for the coke (27% and 145
76 m²/g) together with the high alkalinity indexes of pristine and torrefied lignins
77 compared to that of coal (>27% cf. 0.6%) were considered the main factors that dictated
78 the fast degradation of the biocokes under typical reaction conditions in the blast
79 furnace (>1000 °C, CO₂ atmosphere). Another factor that could lead to the low
80 mechanical strength of the biocoke in blast furnaces could be the smaller graphitization

degree of the carbonized hydrochar compared to coke, as it was suggested for carbonized brown coal [5].

The mineral matter in biomass could be reduced through acid washing. De-ashing pre-treatment of barks of white pine, white spruce and white birch decreased both hydrothermal liquefaction conversion and bio-crude yields, leading to an increase in hydrochar yield [6]. It could be argued that a similar demineralization methodology could be used with lignin in order to increase the hydrochar yield after hydrothermal conversion. The removal of alkaline and alkali earth metals after de-ashing would also lower the reactivity of the resulting biocoke towards CO₂. In industrial coke plants, lignin demineralization could be performed on-site using the sulfuric acid (H₂SO₄) obtained after catalytic conversion of hydrogen sulfide (H₂S), which is recovered in the coke oven gas (COG) treatment plant.

The primary monomers for lignification are *p*-coumaryl alcohol, coniferyl alcohol and sinapyl alcohol. In the lignin polymer, *p*-coumaryl, coniferyl and sinapyl alcohols produce respectively *p*-hydroxyphenyl, guaiacyl and syringyl units [7]. Lignin has a polyphenolic structure that is very similar to that of phenolic resins (Fig. 1). Phenolic resins are synthetic thermosetting polymers with excellent ablative properties and structural integrity [8]. Phenolic resins are synthesized from phenol and formaldehyde using an acid catalyst (novolak type) or a base catalyst (resole type) [9]. The cost of commercial phenolic resins is in the order of \$900–\$1200/ton depending on resin properties and applications [10]. In comparison, the cost of low-grade to high-grade lignins varies from about \$60–\$1350/ton [11] and the cost of premium coking coal has

been in the range of \$200–\$250/ton in 2018. It has been suggested that lignin could be used as a phenol substitute in phenol-formaldehyde resole resins [12], making the cost of phenolic resins competitive if low-value lignins are employed. Indeed, about 50% of Kraft lignin replaced phenol in the synthesis of phenol-formaldehyde resins without substantially modifying the binding properties of the final product [13].

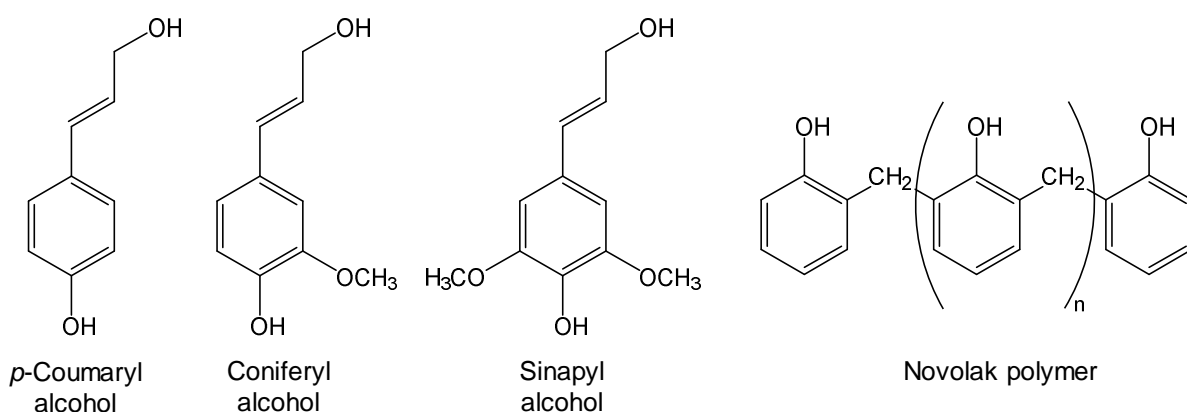


Fig. 1. Chemical structures of primary lignin monomers and novolak polymer [14,15].

The addition of air blown coal tar pitch and phenolic resins (50:50 wt/wt) as binder to coke breeze and anthracite have produced briquettes with high tensile strength even at 950 °C [16,17]. Collin et al. [18] carried out co-carbonization of coal with pitches and waste plastics, including a phenol formaldehyde resin, and it was found that the highest yield of non-volatile compounds was obtained with the reactive pitch containing phenolic resin. In another work, commercial novolak and resole phenol-formaldehyde resins were blended with a coal-tar pitch in order to assess the behavior of the single components and blends upon pyrolysis up to 1000 °C and their reactivity towards CO₂ [19]. These authors found that the burn-off in CO₂ at 1000 °C of the char from resole resin was much higher than that of the char from novolak resin, despite the former

having higher coking value at 550 °C (51.9% cf. 40.8%) and higher carbon yield at 1000 °C (52.1% cf. 32.5%) than the latter. Therefore, the type of phenolic resin can also influence the pyrolysis behavior of the coking blend.

The two main aims of this work are to elucidate whether biocoke can be produced from:

- i) the hydrochar obtained after hydrothermal carbonization of demineralized lignin, and
- ii) blends containing lignin, a low rank (high swelling) poor coking coal and novolak phenolic resin as binding agent.

2. Materials and methods

2.1 Materials

A pine Kraft lignin (L) from the production of cellulose was used in this study. The pine Kraft lignin (also referred to as pristine lignin hereafter) was obtained from Mead-Westvaco (USA) and supplied as a dark brown powder (>99.5% lignin). A commercial novolak phenolic resin patented by Tata Steel Limited and supplied as a yellow powder was used as binding agent. A low rank, high swelling, poor coking bituminous coal (coal A) was selected to prepare blends with lignin and phenolic resin. The ash and volatile matter yields on a dry weight basis of coal A are respectively 9.6 wt% and 33.0 wt%. The coke from coal A was used as reference to evaluate the biocokes from demineralized lignin and blends containing coal A, lignin and phenolic resin.

2.2 Demineralization and torrefaction

The pine Kraft lignin was demineralized in batches using a similar methodology to that used by Fierro et al. [20]. For each batch, 2 L of deionized water was added to 100 g of

lignin, which led to a suspension of pH around 6.8. Afterwards, H₂SO₄ (Acros Organics, 95% solution in water) was gradually added to the lignin suspension until the pH decreased to 1.0. The precipitate was washed gently with deionized water until the pH of the rinse remained constant and close to 6.0. The demineralized lignin (DL) was removed from the suspension by filtration using a Büchner funnel and was dried overnight at 105 °C.

Pristine and demineralized pine Kraft lignins were torrefied at 300 °C under N₂ for 1 h. Torrefaction was carried out by pelletizing approximately 4 g of sample to produce discs of 25 mm in diameter. Eight sample discs were placed inside a ceramic boat and the boat was introduced in the quartz tube reactor of a horizontal tube furnace. A heating rate of 3 °C/min was used from room temperature to the final temperature and a constant N₂ flow of 100 mL/min was used throughout the test. The torrefied lignin (TL) and torrefied demineralized lignin (TDL) were cooled down in N₂ and crushed to particles < 1 mm to prepare the blends for carbonization tests.

2.3 Hydrothermal and standard carbonization tests

Hydrothermal carbonization (HTC) tests have been described in detail in our previous work [4]. Briefly, the equipment comprised of a Parr 4740 series stainless steel 75 mL cylindrical pressure vessel connected to a pressure gauge rated to 690 bar. Heat was applied by means of a fluidized sand bath and the temperature was monitored by means of a K-type thermocouple connected externally to a computer that recorded the temperature every 10 s. Each experiment was conducted with 15 g of demineralized lignin at 350 °C for 6 h using 30 mL of water (biomass/water=0.5 wt/wt). The reactor

was flushed with N₂ to remove the O₂ in the system. The gas generated and the liquid product were discarded and the hydrochar from demineralized lignin (HDL) was recovered and transferred to a vacuum oven where it was dried for 3–4 h at 40 °C.

Standard carbonization tests were carried out in a sole heated oven with the hydrochar from demineralized lignin (HDL) and with blends containing the low rank coking coal A, phenolic resin (PR) and either torrefied lignin (TL) or torrefied demineralized lignin (TDL). For each test, a sample of 80 g with particles <1 mm was compacted in a stainless steel crucible, which was covered with a perforated ceramic top to allow the release of volatiles. The sole in the oven was pre-heated to 1050 °C, and then, the stainless steel crucible configuration containing the sample was placed inside the oven. The sample was heated from the sole at 1050 °C for 2 h. The tests were carried out in inert atmosphere as the volatiles generated by the sample impeded the contact with air.

2.4 Proximate and ultimate analyses

Proximate analysis was carried out following the standard procedures ISO562 and ISO 1171 for humidity, ash and volatile matter determinations. For ultimate analysis, the standard procedures ASTM D5016-98 and ASTM D5373-02 were used for the determination of C, H, N and S using LECO CHN-2000 and LECO S-144DR instruments.

2.5 Solid-state ¹³C nuclear magnetic resonance (NMR)

Cross polarization (CP) coupled with magic angle spinning (MAS) solid-state ¹³C NMR analyses were performed in a Bruker Avance 200 spectrometer at a field strength of 4.7

T, which corresponds to resonance frequencies of 50 MHz for ^{13}C and 200 MHz for ^1H . The samples were packed tightly into a zirconia rotor with a Kel-F rotor-cap and spun at the magic angle ($54^\circ 44'$) with a spinning frequency of approximately 5 kHz. A contact time of 1 millisecond was used during the Hartmann-Hahn condition. The acquisition time was 1.5 s and the spectra were obtained after 2500 scans. The free induction decay (FID) was processed using a line broadening factor of 50 Hz. Tetrakis(trimethylsilyl)silane (TKS), which displays a single peak at 3.5 ppm, was used as internal standard to calibrate the position of the sample peaks.

2.6 Diffuse reflectance infrared Fourier transform spectroscopy (DRIFTS)

DRIFTS spectra were measured using a Nicolet Magna-IR560 spectrometer with a diffuse reflectance accessory. A mercury-cadmium-telluride array (MCT-A) detector that operates at sub-ambient temperature was used. The samples were dried overnight before analysis and the data were collected in the range between $650\text{--}4000\text{ cm}^{-1}$ at a resolution of 4 cm^{-1} . Semi-quantitative analyses were carried out using the integrated area of the absorption bands to calculate selected indices.

2.7 Thermal gravimetric analysis (TGA/DTG)

TGA/DTG of the materials were carried out using a TA Instruments SDT Q600 thermoanalyser. 10–15 mg of sample with particle sizes $<0.212\text{ mm}$ were heated to 1000°C at a rate of $3^\circ\text{C}/\text{min}$ under a N_2 flow of $100\text{ mL}/\text{min}$. From the data obtained, the volatile matter evolved up to a specific temperature (VMT) and in a specific temperature range ($\text{VMT}_1\text{--}\text{T}_2$) and normalized to 100% were calculated. The temperature at 5% conversion (T_i), the temperature at 95% conversion (T_f) and the

temperature of maximum volatile matter evolution (Tmax) were also obtained from the TGA/DTG curves.

2.8 Small amplitude oscillatory shear (SAOS) rheometry

High-temperature SAOS rheometry measurements were performed using a Rheometrics RDA-III high-torque controlled-strain rheometer. The amount of material used for each analysis was 1.5 g. The samples were compacted with a manual hydraulic press under 5 tons of force to form discs of 25 mm in diameter (i.e. around 100 MPa of pressure). The tests involved placing the sample disc between two 25 mm parallel plates, which had serrated surfaces to reduce slippage. Single samples and blends were heated from 50 °C to 500 °C at 3 °C/min. The furnace surrounding the sample was purged with a constant flow of N₂ to transfer heat to the sample and remove the volatiles. The sample temperature was monitored using a thermocouple inside the furnace. A continuous sinusoidal varying strain with amplitude of 0.1% and frequency of 1 Hz (6.28 rad/s) was applied to the sample from the bottom plate throughout the heating period. The stress response on the top plate was measured to obtain the complex viscosity (η^*), which measures the resistance to deformation and flow of the material. The complex viscosity is calculated using Eq. (1), where G' is the storage or elastic modulus, G'' is the loss or viscous modulus and ω is the frequency [21].

$$\eta^*(Pa.s) = \frac{\sqrt{(G')^2 + (G'')^2}}{\omega} \quad (1)$$

2.9 Determination of micro-strength, reactivity and porosity of the biocokes

The micro-strength of the biocokes was determined with the method used by Ragan and Marsh [22]. Briefly, two charges of biocoke (2 g, particle sizes 0.60–1.18 mm) were placed into two separate cylinders of 25.4 mm internal diameter and 305 mm length and sealed by steel dust caps. Each cylinder contained 12 steel ball-bearings of 8 mm in diameter. The samples were subjected to 800 rotations at a speed of 25 rpm. Three indices were derived after sieving: R_1 (>0.6 mm), R_2 (0.6–0.212 mm) and R_3 (<0.212 mm). The higher the value of R_2 and the lower the value of R_3 the higher the micro-strength of the biocoke. At least duplicate tests were performed on each sample.

The reactivity was measured following the ECE-INCAR method [23], which briefly consists of subjecting 7 g of biocoke of particle sizes between 1–3 mm to a CO_2 flow of 120 mL/min at 1000 °C. The reactivity is expressed as the mass loss in percentage terms after 1 h of reaction.

Physical adsorption of CO_2 at 0 °C (273 K) was carried out in a Nova 4200e Quantachrome Instruments to determine the microporous surface area of the biocokes. Degassing was performed in vacuum for 24 h at 200 °C prior to adsorption. The Dubinin-Radushkevich equation was applied to the CO_2 adsorption isotherms in order to obtain the volume of micropores (W_0) and the characteristic adsorption energy (E_0). Following Stoeckli's procedure [24], E_0 was used to calculate the average width of the micropores (L), and then, W_0 and L were used to calculate the surface area of the micropores (S_{mi}) by means of the following empirical equations:

$$L \text{ (nm)} = \frac{10.8}{E_0(\text{kJ/mol}) - 11.4} \quad (2)$$

$$S_{mi} (m^2/g) = \frac{2000 \times W_0 (cm^3/g)}{L (nm)} \quad (3)$$

3. Results and discussion

3.1 Characterization of single materials and blends

Fig. 2 presents the solid-state CP/MAS ^{13}C NMR spectra of pristine pine Kraft lignin (L), pristine lignin demineralized with H_2SO_4 (DL), pristine lignin torrefied in nitrogen at 300 °C for 1 h (TL), demineralized lignin torrefied in nitrogen at 300 °C for 1 h (TDL), demineralized lignin after hydrothermal carbonization (HDL), phenolic resin (PR) and the low rank coking coal (A).

Hagaman and Lee [25] observed that the main differences between the spectra of pristine and demineralized lignins was a loss of the aliphatic signal area centered at 87–70 ppm and an equivalent gain in the area centered at 50–35 ppm in the spectrum of the demineralized lignin. The signal loss was attributed to the spectral region assigned to alcohol functionality (80–70 ppm) and the corresponding gain occurs in the region of highly substituted aliphatic carbon centers. However, the spectra in Fig. 2 do not show significant differences in the peak intensities of pristine and demineralized lignins. The large peak in pristine lignin at around 55 ppm corresponds to methoxyl carbons whereas the large peak at around 147 ppm corresponds to aromatic carbons bonded to methoxy groups [26]. Assuming that the heights of the peaks are directly proportional to their areas, the ratio of aromatic carbons bonded to methoxy groups (Ar–O) to methoxyl carbons (–OCH₃) is 1.3, which is similar to that of demineralized lignin (1.4) but lower than those of both torrefied lignins (1.9).

Torrefaction causes significant changes in the chemical structure of pristine lignin. In our previous work [4], it was found that torrefaction causes complete degradation of aliphatic C–C and C–O groups, polysaccharides, carbonyl and carboxylic acid structures, which were very similar to the modifications caused by hydrothermal carbonization of lignin at 350 °C for 6 h using 30 mL of water. Torrefaction of demineralized lignin greatly reduces the intensity of the peak at around 147 ppm, which corresponds to aromatic carbons bonded to methoxy groups. This leads to a lower ratio of these carbon groups relative to the aromatic C–C and C–H groups positioned at around 130 ppm, which contrasts with the higher ratios in pristine, torrefied or demineralized lignins. From these findings, it can be inferred that demineralization of lignin facilitates the removal of methoxy groups attached to aromatic carbon during torrefaction.

Hydrothermal carbonization of demineralized lignin (350 °C for 6 h using 30 mL of water) completely destroys the methoxy groups in aliphatic structures (55 ppm) and almost destroys all methoxy groups attached to aromatic carbons (147 ppm). The spectrum for the hydrochar (HDL) resembles that of the low rank coal A, although the coal possesses more aliphatic carbon that is evidenced by its lower aromaticity (0.71 cf. 0.85, Table 1).

The spectrum of phenolic resin (PR) is characterized by well-defined peaks and spinning side bands originating from two different aromatic carbons. The peak seen in the 40–30 ppm region originates from carbon in methylene bridges (–CH₂–). However,

315 this peak overlaps the spinning side band originating from aromatic carbon (C–C and
316 C–H) at 130 ppm. The peak at 130 ppm also produces another spinning side band at
317 around 230 ppm. The peak at around 152 ppm corresponds to phenol-ring carbon
318 bearing a hydroxyl group (Ar–OH) and the 122–113 ppm region displays unsubstituted
319 phenol rings (ortho and para) carbons [8,27]. The peak at 152 ppm generates two small
320 spinning side bands, one at around 250 ppm and the other at around 54 ppm. Unlike
321 pine Kraft lignin, the novolak phenolic resin does not show a peak at 55 ppm (i.e. no
322 methoxyl carbons).

323
324 The aromatic and aliphatic carbon peaks in all samples were integrated to calculate the
325 fraction of carbon that is aromatic (Table 1). PR has an aromaticity value of 0.91,
326 which is much higher than those of L, DL, TL and TDL (0.67–0.81). Table 1 also
327 shows that the oxygen content in these five samples varies in a similar manner. It was
328 found that there is an inverse linear correlation between aromaticity values and oxygen
329 content, with coefficient of determination $R^2=0.96$, when the data from DL is omitted.
330 The inclusion of the data from DL reduces the coefficient of determination because
331 demineralization only reduces the oxygen content by 0.4% but increases the aromaticity
332 of lignin from 0.67 to 0.72.

333
334 Fig. 3 shows the DRIFTS spectra of the same samples characterized through solid-state
335 ^{13}C NMR. A series of absorption bands can be appreciated in the spectra. The range
336 between 3700 cm^{-1} and 3100 cm^{-1} is associated to the hydroxyl stretching region.
337 Aromatic and aliphatic stretching C–H appears in the region $3100\text{--}2990\text{ cm}^{-1}$ and
338 $2990\text{--}2795\text{ cm}^{-1}$, respectively. C=O and C=C groups produce peaks in the range

between 1700 cm^{-1} and 1600 cm^{-1} . In addition, peaks at around 1600 cm^{-1} (1), 1510 cm^{-1} (2), 1465 cm^{-1} (3) and 1430 cm^{-1} (4) indicate the existence of aromatic rings and C–H bonds. In the case of lignin samples, the presence of syringyl and guaiacyl groups is evident from the bands at 1370 cm^{-1} (5), and 1270 cm^{-1} (6), respectively. C–O from methoxy groups appears at $1120\text{--}1050\text{ cm}^{-1}$ (7–10). The $900\text{--}700\text{ cm}^{-1}$ range corresponds to out-of-plane vibrations of aromatic C–H [28,29]. Three semi-quantitative indices were calculated to evaluate the chemical changes observed in the infrared spectra of different samples: (i) C=O/C=C index, based on the ratio of the oxygen-containing structures to the aromatic carbon content; (ii) C=O/Hal, ratio of the carbonyl region intensity compared to the aliphatic C–H stretch region intensity; and (iii) H700-900/Hal, ratio of the C–H700-900 out-of-plane deformation compared to the aliphatic C–H stretch region intensity [30].

Fierro et al. [20] found through Fourier transform infrared (FTIR) spectroscopy data analysis that lignin demineralization decreases carbonates (1585 cm^{-1}) and hydroxyl groups ($3600\text{--}3100\text{ cm}^{-1}$) and increases C=O groups (i.e. ketones, aldehydes and carboxyl) not associated with aromatic rings (1729 cm^{-1}). The C=O/C=C index, calculated for L and DL, is in accordance with this observation (0.83 cf. 1.52).

Previous work by our group [4] indicated that lignin torrefaction reduces the intensity of peaks associated to aromatic rings, guaiacyl groups and methoxy groups ($1600\text{--}900\text{ cm}^{-1}$). Torrefaction of either pristine lignin or demineralized lignin produces similar structural changes, as indicated by the almost identical spectra for TL and TDL. The lower amount of aromatic carbons bonded to methoxy groups at 147 ppm in TDL

compared to TL evidenced by solid-state ^{13}C NMR in Fig. 2 could be related to the reduction in C–O from methoxy groups at 1160 cm^{-1} in Fig. 3.

Hydrothermal carbonization of demineralized lignin reduces the amount of hydroxyl groups, aliphatic C–H, $-\text{CH}_2-$ and $-\text{CH}_3$, and increases C=O, aromatic C=C and out-of-plane aromatic C–H. These observations were confirmed by means of the C=O/Hal index (0.85 for L and 1.46 for HDL) and the H700-900/Hal index (0.58 for L and 1.75 for HDL).

From a quantitative point of view and in comparison with all lignin samples, PR is characterized by higher amounts of hydroxyl groups and out-of-plane aromatic C–H and lower amounts of C=O and aliphatic C–H. Low rank coal A possesses less hydroxyl groups, more aromatic and aliphatic C–H, less C=O and more out-of-plane aromatic C–H than the lignin samples. Indeed, the C=O/Hal index of coal A is the lowest (0.29) compared to those calculated for the lignin samples.

Thermogravimetric analysis (TGA) and differential thermogravimetry (DTG) results are presented in Fig. 4. Lignin demineralization decreases the char yield through an enhancement in lignin devolatilization, which is in agreement with previous findings [20,26]. These authors attributed the increase in lignin devolatilization to the removal of sodium and potassium. The derivative curves for TL and TDL overlap throughout the temperature range studied, indicating that torrefaction leads to similar products regardless of whether lignin is in pristine or demineralized form. This is in agreement with DRIFTS results (Fig. 3). However, solid-state ^{13}C NMR results showed that TL

and TDL have different distributions of aromatic carbons bonded to methoxy groups (Fig. 2). Therefore, it could be argued that these methoxy groups degrade into light gases (CH_4 , CO_2 , CO) without causing a significant impact on the devolatilization behavior of the torrefied lignins [31].

The temperature of maximum devolatilization increases in the order: L ($215\text{ }^\circ\text{C}$) < DL ($358\text{ }^\circ\text{C}$) < TL ~ DTL ($407\text{ }^\circ\text{C}$) < coal A ($446\text{ }^\circ\text{C}$) < PR ~ HDL ($511\text{ }^\circ\text{C}$). TL yields higher amount of char at $1000\text{ }^\circ\text{C}$ than PR (63% cf. 57% on a dry and ash free weight basis, Table 1), despite the fact that TL has higher oxygen content (19 wt% cf. 11 wt%) and lower aromaticity (0.79 cf. 0.91) than PR. Table 1 also shows that all lignin samples and PR evolve more volatiles below $400\text{ }^\circ\text{C}$ than coal A. L and DL evolve the highest proportion of volatiles (>65%) below $400\text{ }^\circ\text{C}$. Demineralization of lignin causes a shift in the temperature at 5% conversion (T_i), temperature of maximum volatile release (T_{max}) and temperature at 95% conversion (T_f) to higher values. This results in a lower proportion of volatiles released by DL below $400\text{ }^\circ\text{C}$. As expected from the TGA/DTG curves in Fig. 4, TL and TDL show identical temperatures at 5% and 95% conversions and evolve almost identical amounts of volatiles in the three temperature ranges studied. HDL and PR have similar temperature of maximum volatile release (ca. $511\text{ }^\circ\text{C}$). However, HDL has the lowest temperature at 5% conversion ($175\text{ }^\circ\text{C}$), has the highest temperature at 95% conversion ($845\text{ }^\circ\text{C}$) and produces the highest coke yield in the whole series (69%). PR evolves most volatiles (45%) between $500\text{--}750\text{ }^\circ\text{C}$. In contrast, coal A evolves the highest proportion of volatiles (57%) between $400\text{--}500\text{ }^\circ\text{C}$.

L, DL, TL and TDL were characterized through high-temperature rheometry to elucidate their viscoelastic properties. Fig. 5 shows the variation in complex viscosity (η^*) of the different lignins as a function of temperature. PR is not presented in this figure because the complex viscosity dropped below the detection limit of the instrument once the temperature reached 100 °C, which forced the instrument to abort the test. L shows two minima in complex viscosity (η^*_{\min}), one at around 225 °C and the other at around 350 °C. Demineralization of lignin does not affect the generation of fluid entities at 225 °C but increases the fluidity at 350 °C, as indicated by the lower minimum complex viscosity value for DL. Torrefaction destroys the fluid entities regardless of whether lignin is in pristine form (TL) or demineralized form (TDL).

Blends of pristine or torrefied lignin with phenolic resin were also characterized through high-temperature rheometry (Fig. 5). Blends of L and PR show that the viscoelastic behavior of the blend is controlled by lignin. PR interacts with L above 200 °C and causes an exponential reduction in maximum fluidity at 225 °C with coefficient of determination $R^2 > 0.99$. A reduction in the maximum fluidity at 350 °C is also observed but the exponential correlation has lower coefficient of determination ($R^2 = 0.92$).

Blends of TL and PR do not develop fluidity since the complex viscosity increases and remains above 10^6 Pa.s above 150 °C, which is characteristic of predominantly solid-like materials. Usually, the higher the amount of phenolic resin in the blend the higher the complex viscosity values. At 300–550 °C, condensation reactions involving methylene and hydroxyl functional groups dominate during phenolic resin pyrolysis, which lead to carbon-hydrogen crosslinks [32]. These crosslinks will increase the viscosity of PR, and thus, the viscosity of the blend with TL. It was observed that the

semichars obtained at the end of the rheometry tests with both blends (L-PR and TL-PR) presented good cohesion when the concentration of L in the blend was ≤ 60 wt% and the concentration of TL in the blend was ≤ 80 wt%. Since TL possesses higher porosity than L, it is thought that the higher contact area between TL and PR particles favors higher cohesion, allowing for higher amounts of TL in the blend than with L. Therefore, more lignin can be included in blends with PR if lignin is in torrefied form (up to 80 wt%). It has to be noted that semichars are intermediate products and this work is mainly focusing on the final biocoke product. For this reason, no attempt was made to determine the mechanical strength of the different semichars obtained.

3.2 Characterization of the hydrochar and biocoke from demineralized lignin

The composition and yield of the hydrochar obtained from demineralized lignin after hydrothermal carbonization at 350 °C for 6 h using 30 mL of water (HDL) are presented in Table 2. Data for the hydrochars from pristine lignin (HL) and torrefied lignin (HTL) are also shown for comparison purposes. Our previous work [4] found that the biocoke produced from HTL did not agglomerate, contrary to the behavior of biocokes produced at 1050 °C from HL and a 50:50 wt/wt blend of HL and HTL. In the case of the hydrochar obtained here from demineralized lignin, it was found that the biocoke obtained showed agglomeration. Compared to HL, HDL yields lower ash (0.4 wt% cf. 1.0 wt%) and has lower nitrogen (0.6 wt% cf. 1.1 wt%) and oxygen (10.6 wt% cf. 11.5 wt%) contents. Moreover, the hydrochar yield from DL (57%) is lower than that from L (61%). Ash promotes hydrochar formation and the reduction in ash yield from DL might be responsible for the lower hydrochar yield. The biocoke yields obtained from HL and HDL are fairly similar but lower than the biocoke yield obtained from HTL (ca.

68% cf. 73%). The overall biocoke yields from pristine, demineralized and torrefied lignins, taking into account the yields from hydrothermal carbonization (HL, HDL and HTL), are around 41%, 39% and 62%, respectively. Therefore, demineralization does not have a significant impact on biocoke yield and will preserve biocoke agglomeration.

The micro-strength indices (R_1 , R_2 and R_3) and reactivity of the biocokes derived from HL and HDL are presented in Table 3. The values for HTL are not presented because its biocoke did not agglomerate. The value of R_1 (percentage of particles >0.6 mm) is comparable in both biocokes but R_2 (percentage of particles between 0.6–0.212 mm) is higher and R_3 (percentage of particles <0.212 mm) is lower in the biocoke from HDL. These results indicate that the biocoke derived from HDL has higher mechanical strength than the biocoke from HL. However, the mechanical strength of the biocoke from HDL is lower than that of the coke from coal A, as indicated by the higher value of R_3 (46.0% cf. 39.7%).

In addition, the reactivity of the biocoke derived from HDL is 20% lower than the reactivity of the biocoke derived from HL. This contrasts with the higher microporous surface area of the biocoke from HDL compared to that of the biocoke from HL ($477 \text{ m}^2/\text{g}$ cf. $414 \text{ m}^2/\text{g}$, Table 3). Still, the reactivity of the biocoke from HDL (25.5%) is significantly high compared to the reactivity of the coke from coal A (11.2%). Therefore, demineralization of lignin improves the reactivity of the biocoke but this improvement is not enough for blast furnace utilization.

3.3 Characterization of biocokes from blends containing coal, lignin and phenolic resin

As previously mentioned, more lignin can be blended with phenolic resin if it is in torrefied form (up to 80 wt%). Moreover, the char yield of torrefied lignin is higher than that of pristine lignin (63% cf. 37%, Table 1). Therefore, torrefied lignin (TL) and phenolic resin (PR) were combined with the low rank, high swelling, poor coking coal (A) in order to formulate a blend that can perform like a good coking coal during carbonization.

The use of the phenolic resin as a binder in the blend must be minimized due to its elevated cost. Therefore, the ratio of torrefied lignin to phenolic resin should be kept at 4:1 wt/wt in order to achieve good cohesion of the semichar, as previously determined. Lower amounts of phenolic resin (i.e. < 20 wt%) would lead to poor cohesion with torrefied lignin and produce brittle semichars and biocokes.

In addition, the amount of coal A must be tailored to achieve a suitable level of fluidity in the blend since phenolic resin and torrefied lignin will reduce the amount of fluid material evolving from the coal. If the amount of coal A in the blend is too high, the resulting high fluidity of the blend will lead to excessive porosity that will impact the mechanical strength of the biocoke. If the amount of coal A in the blend is too low, torrefied lignin and phenolic resin will completely destroy fluidity development in the coal and the biocoke will not possess sufficient porosity to allow gas permeability inside the blast furnace.

In order to determine the optimum composition of this ternary blend (coal, phenolic resin and torrefied lignin), the viscoelastic and expansion/collapse behaviors of coal A

and two blends with different compositions were characterized through high-temperature SAOS rheometry (Fig. 5). The results show that coal A develops a minimum in complex viscosity of about 600 Pa.s at 430 °C. Simultaneously, the coal mass undergoes expansion and significant collapse, which represent 6% and 92% of initial disc thickness, respectively. The addition of PR and TL to coal A causes a reduction in fluidity (i.e. increase in minimum complex viscosity) and also an increase in the temperature of maximum fluidity to 440–445 °C. Indeed, the blend containing 75 wt% of coal A shows expansion and significant collapse (8% and 75% of initial disc thickness, respectively) that resembles the behavior of coal A alone. The expansion/collapse behavior is directly related to the high fluidity of this blend, as indicated by its low η^*_{\min} value of 3×10^3 Pa.s (high fluidity coking coals develop η^*_{\min} values around 10^3 Pa.s). The blend produced a highly porous and brittle semicoke at 500 °C, which was glued to the parallel plates of the rheometer. In contrast, the blend containing 70 wt% of coal A develops fluidity at around 445 °C ($\eta^*_{\min}=10^5$ Pa.s), does not expand and collapses slightly (only 15% of initial disc thickness). It was also found that the semicoke obtained at 500 °C showed good cohesion and was easily removed from the parallel plates of the rheometer, which are typical features of semicokes derived from good coking coals. No attempt was made to determine the mechanical strength of these semicokes since they are intermediate products. Based on these results, the blend containing 70 wt% of coal A was chosen for a carbonization test at 1050 °C in the sole heated oven. The mechanical strength, reactivity and microporous surface area of the resulting biocoke was determined and the results are presented in Table 3. The fraction of fines (R_3) generated by the biocoke (27.2%) is lower than that generated by the coke from the coal A (39.7%). Moreover, the value of R_2 is higher in

the biocoke than in the coke (70.2% cf. 50.0%). Therefore, these results indicate that the biocoke has higher mechanical strength than the coke. However, the reactivity of the biocoke (20.8%) is much higher than that of the coke (11.2%). Table 3 also shows that replacement of torrefied lignin (TL) with torrefied demineralized lignin (TDL) does not affect the mechanical strength of the biocoke but lowers its reactivity from 20.8% to 16.7% and increases the microporous surface area by 35 m²/g. These results indicate that there is no evident relationship between the microporous surface area of the biocoke and biocoke reactivity. The biocoke yield of the A/PR/TDL blend was calculated using the coke yields in Table 1 for each component. The biocoke yield of the blend (66%) is comparable to the coke yield of coal A (68%).

Arguably, the partial replacement of the coal A with a petroleum coke with low reactivity [33] could further reduce the reactivity of the biocoke. Obviously, the addition of this carbonaceous additive will impact fluidity development, and thus, the combined percentage of TDL and PR must be reduced below 30 wt% to preserve the fluid properties of the blend. Further research would be necessary to demonstrate whether the addition of petroleum coke could reduce the reactivity of the blend to levels suitable for blast furnace operation and to evaluate the economic viability of producing such blends.

4. Conclusions

The biocoke obtained after carbonization at 1000 °C from the hydrochar of demineralized lignin had much higher reactivity than the coke obtained from a low rank coking coal (26% cf. 11%), proving that lignin demineralization cannot improve the

biocoke quality to levels that fulfil blast furnace requirements. In another approach, blends of high swelling coal (70 wt%), torrefied lignin before or after demineralization (24 wt%) and phenolic resin (6 wt%) produced biocokes with suitable mechanical strength for handling but still showed excessive reactivity (>16%) compared to the coke from the low rank coal (11%). No obvious relationship between biocoke reactivity and its microporous surface area was found.

Acknowledgements

This research did not receive any specific grant from funding agencies in the public, commercial, or not-for-profit sectors. The authors thank MeadWestvaco for supplying the pine Kraft lignin and Tata Steel Limited for providing the phenolic resin used in this study.

References

- [1] Suopajarvi H, Umeki K, Mousa E, Hedayati A, Romard H, Kemppainen A, Wang C, Phounglamcheik A, Tuomikoski S, Norberg N, Andefors A, Öhman M, Lassi U, Fabritius T. Use of biomass in integrated steelmaking – Status quo, future needs and comparison to other low-CO₂ steel production technologies. Appl Energ 2018;213:384–407. <https://doi.org/10.1016/j.apenergy.2018.01.060>.
- [2] Xing X, Rogers H, Zhang G, Hockings K, Zulli P, Deev A, Mathieson J, Ostrovski O. Effect of charcoal addition on the properties of a coke subjected to simulated blast furnace conditions. Fuel Process Technol 2017;157:42–51. <https://doi.org/10.1016/j.fuproc.2016.11.009>.

- 577 [3] Suopajarvi H, Dahl E, Kemppainen A, Gornostayev S, Koskela A, Fabritius T.
578 Effect of charcoal and Kraft-lignin addition on coke compression strength and
579 reactivity. *Energies* 2017;10:1850–64. <https://doi.org/10.3390/en10111850>.
- 580 [4] Castro-Díaz M, Uguna CN, Florentino L, Díaz-Faes E, Stevens LA, Barriocanal C,
581 Snape CE. Evaluation of hydrochars from lignin hydrous pyrolysis to produce
582 biocokes after carbonization. *J Anal Appl Pyrol* 2017;124:742–51.
583 <https://doi.org/10.1016/j.jaap.2016.11.010>.
- 584 [5] Mollah MM, Marshall M, Jackson WR, Chaffee AL. Attempts to produce blast
585 furnace coke from Victorian brown coal. 2. Hot briquetting, air curing and higher
586 carbonization temperature. *Fuel* 2016;173:268–76.
587 <https://doi.org/10.1016/j.fuel.2016.01.053>.
- 588 [6] Feng S, Yuan Z, Leitch M, Xu CC. Hydrothermal liquefaction of barks into bio-
589 crude - Effects of species and ash content/composition. *Fuel* 2014;116:214–20.
590 <https://doi.org/10.1016/j.fuel.2013.07.096>.
- 591 [7] Ralph J, Lundquist R, Brunow G, Lu F, Kim H, Schatz PF, Marita JM, Hatfield
592 RD, Ralph SA, Christensen JH, Boerjan W. Lignins: Natural polymers from
593 oxidative coupling of 4-hydroxyphenylpropanoids. *Phytochem Rev* 2004;3:29–60.
594 <https://doi.org/10.1023/B:PHYT.0000047809.65444.a4>.
- 595 [8] Ottenbours B, Adriaenssens B, Carleer R, Vanderzande D, Gelan J. Quantitative
596 carbon-13 solid-state n.m.r. and FT-Raman spectroscopy in novolac resins.
597 *Polymer* 1998;39:5293–300. [https://doi.org/10.1016/S0032-3861\(97\)10283-X](https://doi.org/10.1016/S0032-3861(97)10283-X).
- 598 [9] Pilato L. Phenolic resins: 100 Years and still going strong. *React Funct Polym*
599 2013;73:270–7. <https://doi.org/10.1016/j.reactfunctpolym.2012.07.008>.

- [10] Ashby M, Johnson K. Materials and design: The art and science of material selection in product design. 3rd ed. Oxford: Butterworth-Heinemann; 2014.
- [11] Laurichesse S, Avérous L. Chemical modification of lignins: Towards biobased polymers. Prog Polym Sci 2014;39:1266–90.
<https://doi.org/10.1016/j.progpolymsci.2013.11.004>.
- [12] Alonso MV, Oliet M, Pérez JM, Rodríguez F, Echeverría J. Determination of curing kinetic parameters of lignin–phenol–formaldehyde resol resins by several dynamic differential scanning calorimetry methods. Thermochim Acta 2004;419:161–7. <https://doi.org/10.1016/j.tca.2004.02.004>.
- [13] García Calvo-Flores F, Dobado JA. Lignin as renewable raw material. ChemSusChem 2010;3:1227–35. <https://doi.org/10.1002/cssc.201000157>.
- [14] Deuss PJ, Barta K. From models to lignin: Transition metal catalysis for selective bond cleavage reactions. Coordin Chem Rev 2016;306:510–32.
<https://doi.org/10.1016/j.ccr.2015.02.004>.
- [15] Tennison SR. Phenolic-resin-derived activated carbons. Appl Catal A-Gen 1998;173:289–311. [https://doi.org/10.1016/S0926-860X\(98\)00186-0](https://doi.org/10.1016/S0926-860X(98)00186-0).
- [16] Benk A. Utilisation of the binders prepared from coal tar pitch and phenolic resins for the production metallurgical quality briquettes from coke breeze and the study of their high temperature carbonization behaviour. Fuel Process Technol 2010;91:1152–61. <https://doi.org/10.1016/j.fuproc.2010.03.030>.
- [17] Benk A, Coban A. Investigation of resole, novalac and coal tar pitch blended binder for the production of metallurgical quality formed coke briquettes from coke breeze and anthracite. Fuel Process Technol 2011;92:631–8.
<https://doi.org/10.1016/j.fuproc.2010.11.022>.

- [18] Collin G, Bujnowska B, Polaczek J. Co-coking of coal with pitches and waste plastics. *Fuel Process Technol* 1997;50:179–84. [https://doi.org/10.1016/S0378-3820\(96\)01068-5](https://doi.org/10.1016/S0378-3820(96)01068-5).
- [19] Machnikowski J, Rutkowski P, Diez MA. Co-treatment of novolac- and resole-type phenolic resins with coal-tar pitch for porous carbons. *J Anal Appl Pyrol* 2006;76:80–7. <https://doi.org/10.1016/j.jaap.2005.08.003>.
- [20] Fierro V, Torné-Fernández V, Celzard A, Montané D. Influence of the demineralisation on the chemical activation of Kraft lignin with orthophosphoric acid. *J Hazard Mater* 2007;149:126–33. <https://doi.org/10.1016/j.jhazmat.2007.03.056>.
- [21] Steel KM, Castro-Díaz M, Patrick JW, Snape CE. Use of rheometry and ¹H NMR spectroscopy for understanding the mechanisms behind the generation of coking pressure. *Energ Fuel* 2004;18:1250–6. <https://doi.org/10.1021/ef034058l>.
- [22] Ragan S, Marsh H. Carbonization and liquid-crystal (mesophase) development. 22. Micro-strength and optical textures of cokes from coal-pitch co-carbonizations. *Fuel* 1981;60:522–8. [https://doi.org/10.1016/0016-2361\(81\)90116-2](https://doi.org/10.1016/0016-2361(81)90116-2).
- [23] Menendez JA, Alvarez R, Pis JJ. Relationship between different methods of determination of coke reactivity (Spanish). *Revista de Metalurgia* 1993;29:214–22.
- [24] Stoeckli F. Characterization of microporous carbons by adsorption and immersion techniques. In: Patrick JW, editor. *Porosity in Carbons*, London: Edward Arnold; 1995, p. 67–92.
- [25] Hagaman EW, Lee SK. Acid-catalyzed cross-linking reactions at benzylic sites in fluorene monomers, polymers, and lignin. *Energ Fuel* 1999;13:1006–14. <https://doi.org/10.1021/ef980269s>.

- [26] Sharma RK, Wooten JB, Baliga VL, Lin X, Chan WG, Hajaligol MR. Characterization of chars from pyrolysis of lignin. *Fuel* 2004;83:1469–82. <https://doi.org/10.1016/j.fuel.2003.11.015>.
- [27] Maciel GE, Chuang I-S, Gollob L. Solid-state ^{13}C NMR study of resol-type phenol-formaldehyde resins. *Macromolecules* 1984;17:1081–7. <https://pubs.acs.org/doi/10.1021/ma00135a018>.
- [28] Liu Q, Wang S, Zheng Y, Luo Z, Cen K. Mechanism study of wood lignin pyrolysis by using TG-FTIR analysis. *J Anal Appl Pyrol* 2008;82:170–7. <https://doi.org/10.1016/j.jaap.2008.03.007>.
- [29] Kang S, Li X, Fan J, Chang J. Characterization of hydrochars produced by hydrothermal carbonization of lignin, cellulose, D-xylose, and wood meal. *Ind Eng Chem Res* 2012;51:9023–31. <https://doi.org/10.1021/ie300565d>.
- [30] Chen Y, Mastalerz M, Schimmelmann A. Characterization of chemical functional groups in macerals across different coal ranks via micro-FTIR spectroscopy. *Int J Coal Geol* 2012;104:22–3. <https://doi.org/10.1016/j.coal.2012.09.001>.
- [31] Zhao J, Xiuwen W, Hu J, Liu Q, Shen D, Xiao R. Thermal degradation of softwood lignin and hardwood lignin by TG-FTIR and Py-GC/MS. *Polym Degrad Stabil* 2014;108,133–8. <https://doi.org/10.1016/j.polymdegradstab.2014.06.006>.
- [32] Trick KA, Saliba TE. Mechanisms of the pyrolysis of phenolic resin in carbon/phenolic composite. *Carbon* 1995;33:1509–15. [https://doi.org/10.1016/0008-6223\(95\)00092-R](https://doi.org/10.1016/0008-6223(95)00092-R).
- [33] Alvarez R, Pis JJ, Díez MA, Barriocanal C, Canga CS, Menéndez JA. A semi-industrial scale study of petroleum coke as an additive in cokemaking. *Fuel Process Technol* 1998;55:129–41. [https://doi.org/10.1016/S0378-3820\(97\)00078-7](https://doi.org/10.1016/S0378-3820(97)00078-7).

Table 1. Proximate analysis, ultimate analysis, aromaticity and parameters derived from thermogravimetric analysis of pine Kraft lignin (L), demineralized lignin (DL), torrefied lignin (TL), torrefied demineralized lignin (TDL), hydrochar from demineralized lignin (HDL), phenolic resin (PR) and low rank coking coal (A). Weight percentages are expressed either on a dry basis (db) or on a dry ash-free basis (daf).

Parameter	L	DL	TL	TDL	HDL	PR	A
Ash (wt%, db)	2.5	0.6 ^a	3.1	0.9	0.4	0.0 ^a	9.6
VM (wt%, db)	64.0	60.9 ^a	38.7	36.2	30.2	44.3 ^a	33.0
C (wt%, db)	64.7	66.6	73.5	76.2	83.2	78.5	78.5
H (wt%, db)	5.7	5.8	4.8	4.7	4.5	5.9	5.0
N (wt%, db)	0.9	0.5	0.7	0.6	0.6	4.6	1.6
S (wt%, db)	1.5	1.2	1.1	0.7	0.7	0.0	1.1
O ^b (wt%, db)	26.3	25.3	19.0	16.9	10.6	11.0	4.2
Aromaticity ^c	0.67	0.72	0.79	0.81	0.85	0.91	0.71
Ti (°C)	187	211	290	292	175	199	319
Tf (°C)	628	669	814	815	845	722	761
Tf–Ti (°C)	441	458	524	523	670	523	442
VM400 (%)	74.1	66.8	26.5	26.1	37.0	29.0	16.3
VM400–500 (%)	13.3	17.0	31.1	31.3	18.4	25.9	57.4
VM500–750 (%)	10.5	13.4	34.1	34.4	35.1	41.3	20.8
DTGmax (%/min)	0.89	1.08	0.43	0.43	0.21	0.66	0.85
Tmax (°C)	215	358	407	405	510	512	446
Coke yield (% , daf)	37.0	36.2	63.0	63.4	69.0	57.3	68.1

^a Thermogravimetric data.

^b By difference.

^c Error of ± 1 in absolute values.

Table 2. Proximate analysis, ultimate analysis, mean hydrochar yield and standard deviation values calculated from different hydrothermal carbonization tests, and biocoke yield of the hydrochars from pine Kraft lignin (HL), demineralized lignin (HDL) and torrefied lignin (HTL). Weight percentages are expressed on a dry basis (db).

Parameter	HL	HDL	HTL
Ash (wt%, db)	1.0	0.4	1.7
VM (wt%, db)	31.2	30.2	25.8
C (wt%, db)	82.0	83.2	81.6
H (wt%, db)	4.6	4.5	4.1
N (wt%, db)	1.1	0.6	0.9
S (wt%, db)	0.8	0.7	0.9
O ^a (wt%, db)	11.5	10.6	12.5
Hydrochar yield, mean (%)	60.7	56.5	84.3
Standard deviation	3.3	1.4	1.3
Number of HTC tests	14	12	16
Biocoke yield (%)	67	69	73

^a By difference.

688

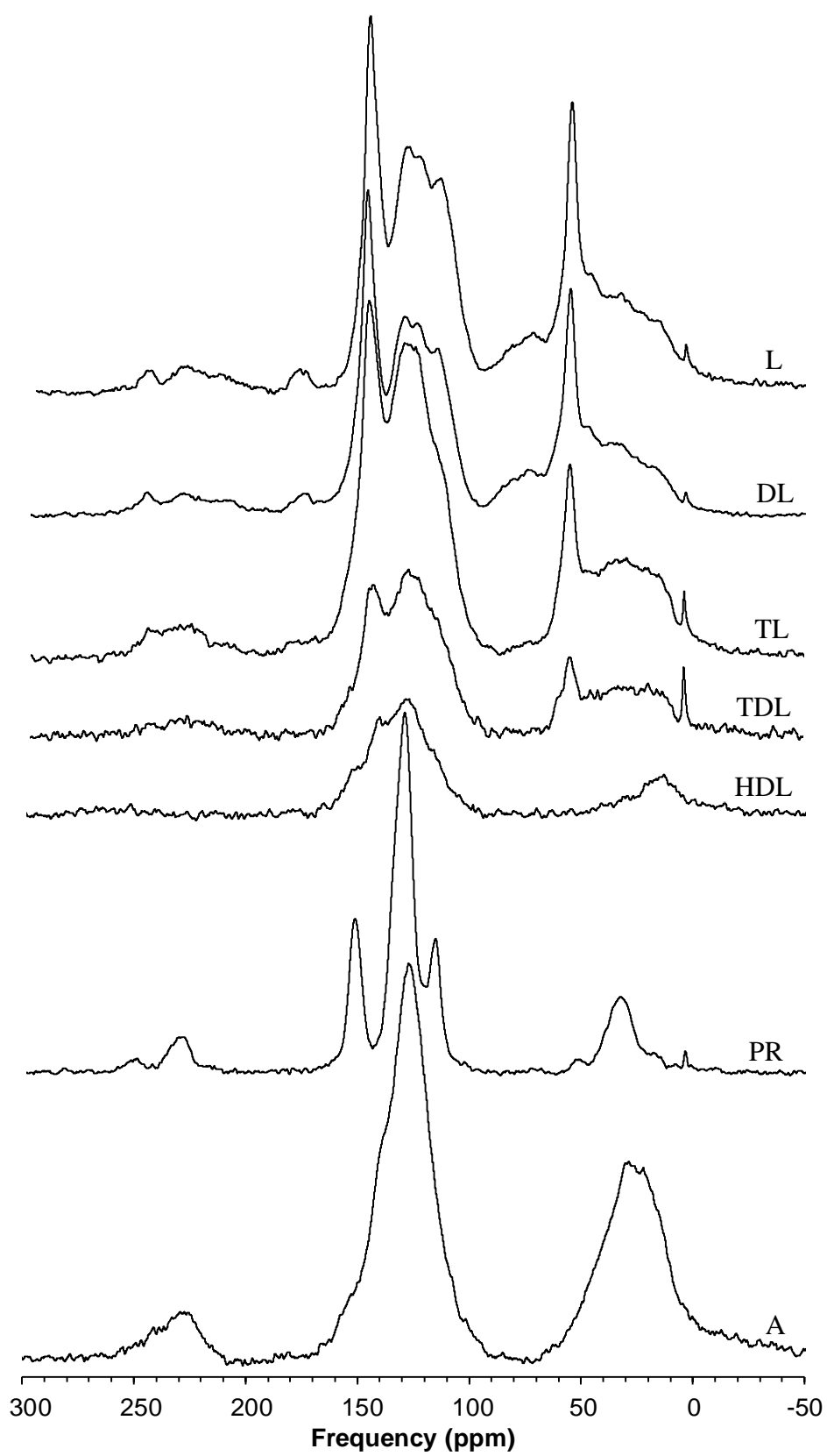
689 Table 3. Micro-strength indices, reactivity values and microporous surface areas of the
 690 biocokes obtained from the hydrochars from pristine lignin (HL) and demineralized
 691 lignin (HDL), two blends containing 70 wt% low rank coal (A), 24 wt% torrefied lignin
 692 (TL) or torrefied demineralized lignin (TDL) and 6 wt% phenolic resin (PR) and the
 693 coke from the low rank coking coal (A).

694

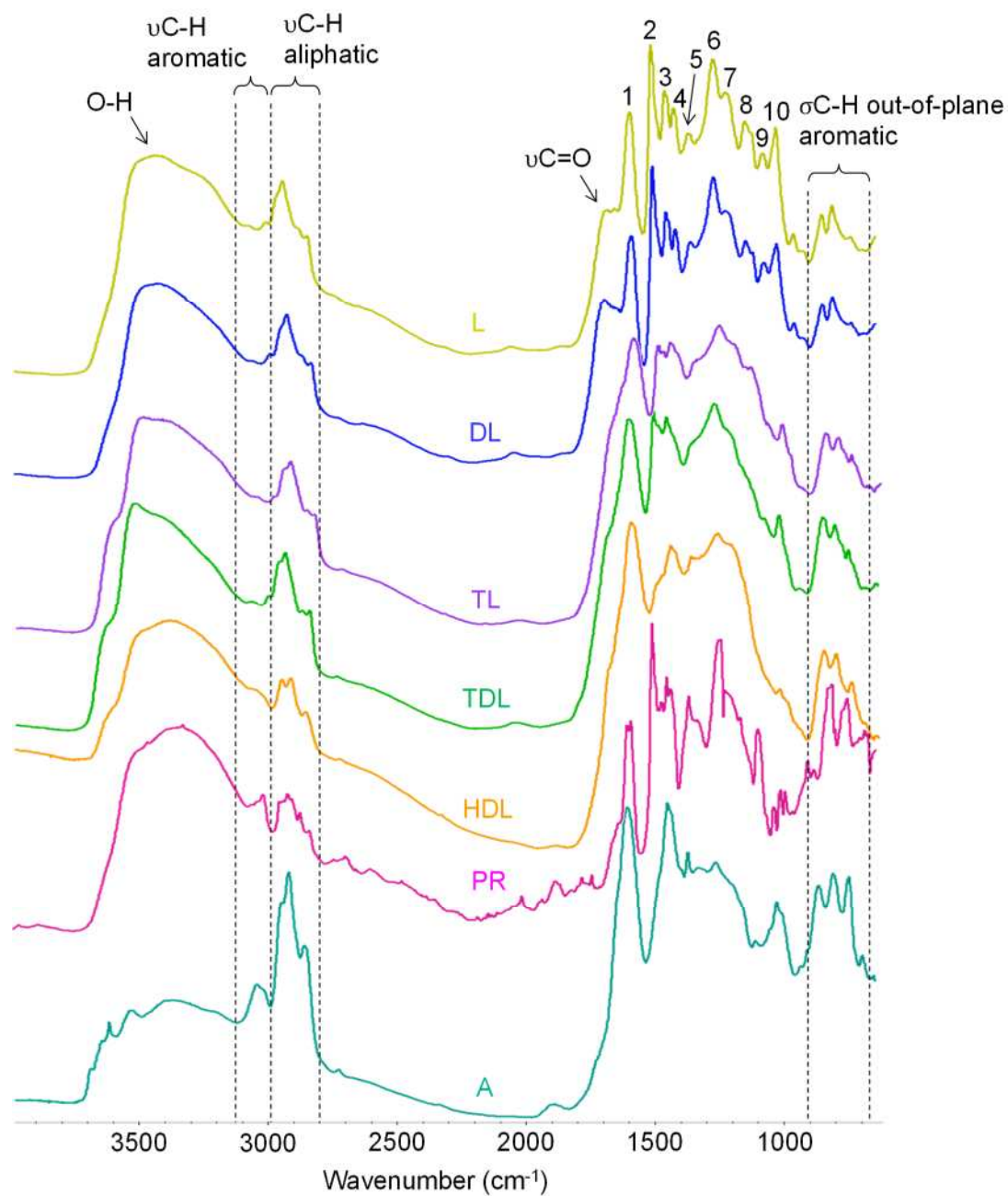
Parameter	Biocoke (HL)	Biocoke (HDL)	Biocoke (A/PR/TL)	Biocoke (A/PR/TDL)	Coke (A)
R ₁ (%)	0.4	0.3	2.6	3.3	10.4
R ₂ (%)	30.6	53.7	70.2	69.4	50.0
R ₃ (%)	69.0	46.0	27.2	27.3	39.7
Reactivity (%)	45.1	25.5	20.8	16.7	11.2
S _{mi} (m ² /g)	414	477	115	150	20

695 The standard deviation for the values of R₁, R₂, R₃ and reactivity are respectively 0.9,
 696 2.8, 2.0 and 0.3.

697



699 Fig. 2. CP/MAS ^{13}C NMR spectra of pine Kraft lignin (L), demineralized lignin (DL),
700 torrefied lignin (TL), torrefied demineralized lignin (TDL), hydrochar from
701 demineralized lignin (HDL), phenolic resin (PR) and low rank coking coal (A). The
702 peak at 3.5 ppm corresponds to the internal standard tetrakis(trimethylsilyl)silane
703 (TKS).
704



706

707 Fig. 3. DRIFTS spectra of pine Kraft lignin (L), demineralized lignin (DL), torrefied
 708 lignin (TL), torrefied demineralized lignin (TDL), hydrochar from demineralized lignin
 709 (HDL), phenolic resin (PR) and low rank coking coal (A).

710

711

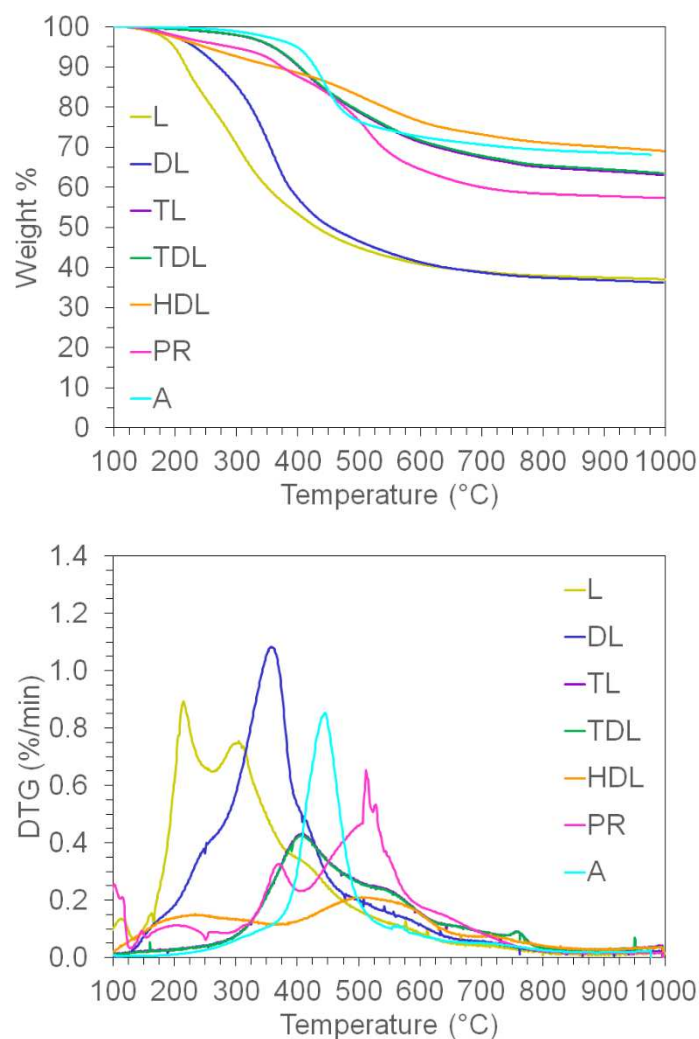
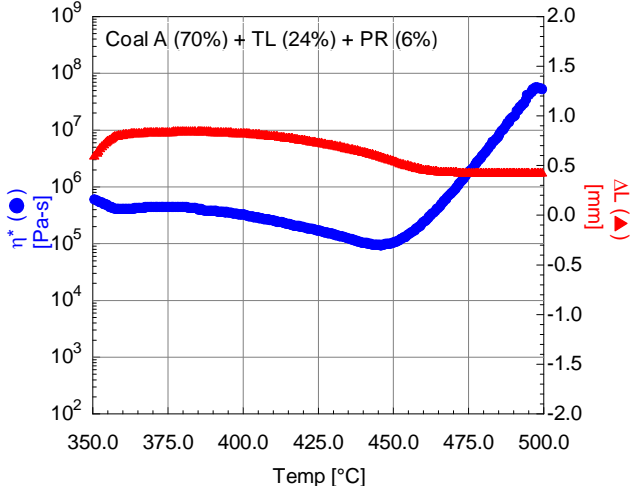
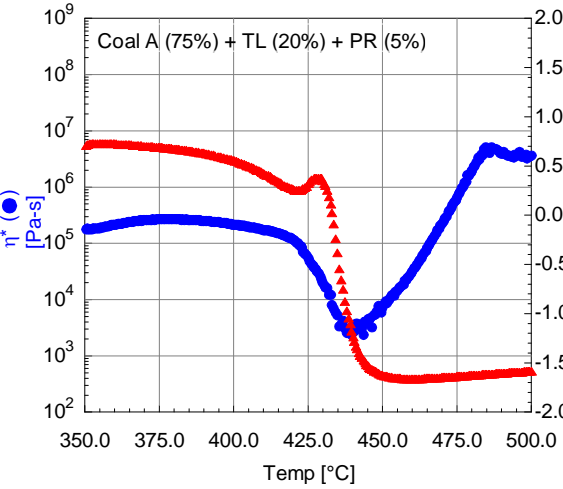
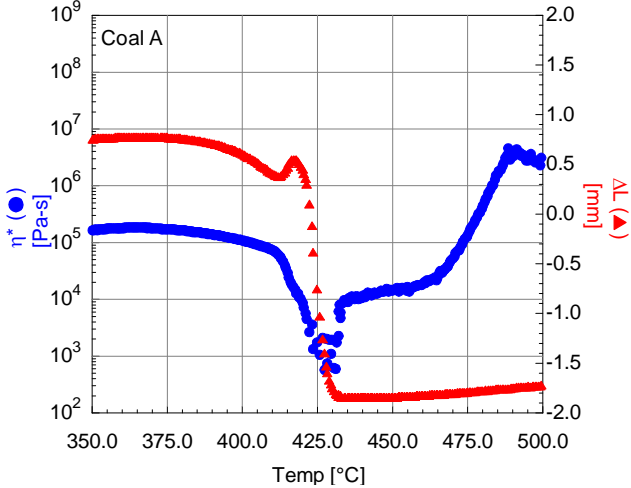
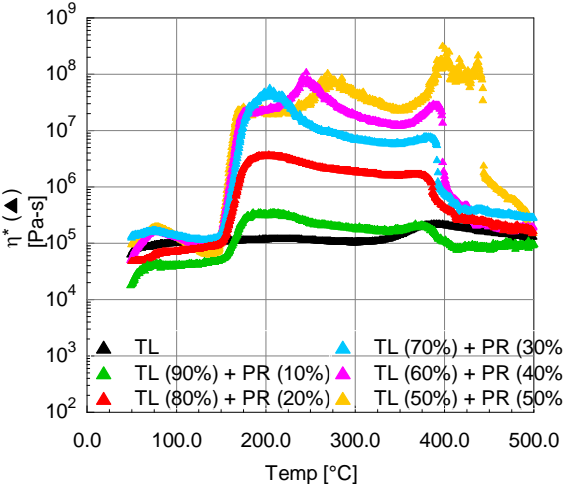
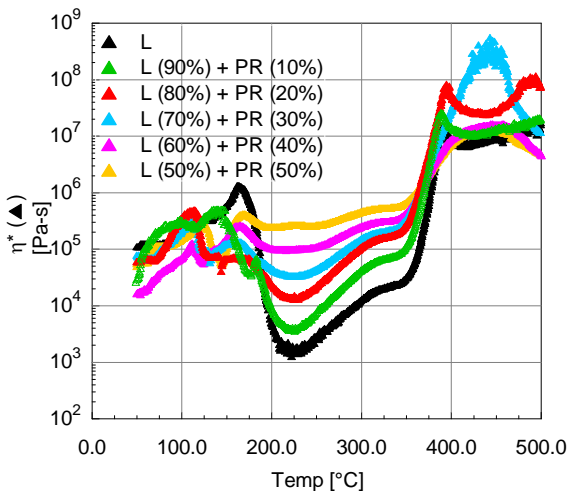
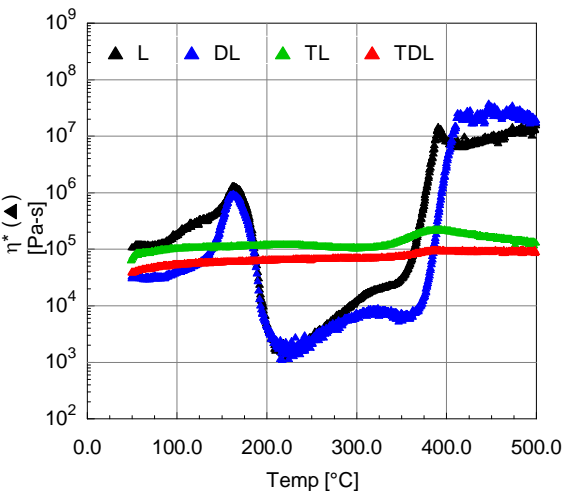


Fig. 4. Weight percentage and derivative of weight percentage as a function of temperature for pine Kraft lignin (L), demineralized lignin (DL), torrefied lignin (TL), torrefied demineralized lignin (TDL), hydrochar from demineralized lignin (HDL), phenolic resin (PR) and low rank coking coal (A).



723 Fig. 5. Complex viscosity (η^*) as a function of temperature for pine Kraft lignin (L),
724 demineralized lignin (DL), torrefied lignin (TL), torrefied demineralized lignin (TDL)
725 and blends of pristine and torrefied lignins with phenolic resin (PR) of different weight
726 compositions, and complex viscosity (η^*) and plate gap (ΔL) as a function of
727 temperature for low rank coking coal A and two blends of coal A, TL and PR of
728 different weight compositions.